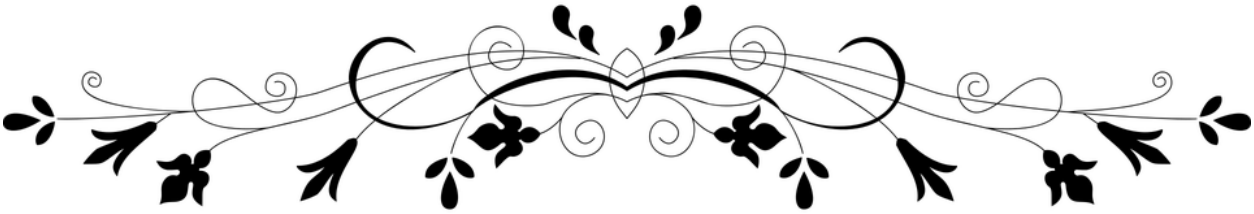

CHAPTER 6

Lattice-Strain induced photo-physical properties of $NaYF_4$: Yb^{3+}, Tm^{3+} Upconverting phosphors

CHAPTER 6

6.1 Introduction

The multiple usability Yb^{3+}-Tm^{3+} co-doped $NaYF_4$ Upconverting phosphors in the field of cancer theranostics and other diverse area like magnetism require their size as well as morphology tunability [371-373]. Further, the dynamics of the entire Upconversion process to optimize the resulting luminescence intensity is bestowed upon one important crystallographic parameter, "lattice strain" [374, 375]. Generally, during hydrothermal growth of Upconverting phosphors, doped rare-earth ions substitute the Y^{3+} ions of the host lattice resulting lattice distortion in terms of strain. Lattice strain-induced alters energy levels of bonding electrons, hence there is variation in the photoluminescence intensity [376, 377]. Generally the parity forbidden transitions and non-radiative phonon relaxation, result in low Upconversion efficiency. These problem can be overcome by adjusting local crystal field symmetry around doped rare-earth ions and increasing the rate of energy transfer between the sensitizer and activator pair. Under such circumstances lattice strain is crucial, responsible for distortion of crystal field and minimization of phonon relaxation. Therefore, it is crucial to ascertain the lattice strain developed in crystal structure and its quantification.

It is understood that chelating agents and substrates used during hydrothermal synthesis collectively play a cardinal role in inducing strain in the developing crystals [378-382] besides phase, morphology and crystallinity control. Utilizing this acquaintance, it will be interesting to investigate the change in morphology, crystallinity, and photo-physical property of Upconverting phosphors as a function of the substrate and chelating agents interlinked with lattice strain. These imperative studies enable us for development of high

quality Upconverting phosphors with assorted morphology, dimension and photo-physical properties for multifunctional applications. Moreover, this type of modified synthesis strategy also surfaced from the fact that nowadays $NaYF_4$ Upconverting phosphors exhibited great demand in several specific optical sectors [383-386] which require their efficient growth over various charged/un-charged substrates in a facile manner using hydrothermal method. Technically the dipped substrates in the precursor solution provide simultaneous nucleation sites for the growth of Upconverting phosphors [387, 388]. The initial seed formed on a substrate subsequently developed into a full-grown crystal following the classical growth mechanism but sheared off into the bulk solution via continuously stirring precursor. Successive to that growth of Upconverting crystals consummate through dissolution recrystallization mechanism resembling digestive ripening process and finally stabilized over dipped substrate. Therefore, Upconverting film growth is probably a two-way process, and it is essential to investigate the particles formed in the bulk phase.

Hence the objective of this study to synthesizing Yb^{3+}-Tm^{3+} co-doped $NaYF_4$ Upconverting phosphors (UCP) with varying morphology and emission characteristics using the hydrothermal technique as function of substrate and chelating agents. Further, to evaluate their synergistic role in controlling the crystallinity, morphology, and emission property of Upconverting phosphors related with the lattice strain.

6.2 Experimental

6.2.1 Materials Required

Yttrium chloride hexahydrate ($YCl_3.6H_2O$, 99.99%) and Thulium chloride hexahydrate ($TmCl_3.6H_2O$, 99.99%) were purchased from Sigma Aldrich, while Ytterbium chloride hexahydrate ($YbCl_3.6H_2O$, 99.99%) was purchased from Otto Chemicals. Sodium Fluoride (NaF, 99.99, Ethylene diamine tetra acetate (EDTA, 99.99%), Diethylene triamine penta acetic acid (DTPA, 99.99%), Ethylene glycol tetra-acetic acid (EGTA, 99.99%) were purchased from SRL Chemicals. Indium-doped Tin oxide (ITO), Fluorine doped Tin oxide (FTO), and plain silica glass (P.G.) substrates were obtained from Techinstro Pvt. Ltd., India. Hydrofluoric acid (HF, Merck Life Science Pvt. Ltd. Mumbai) was used for etching purposes. All the chemicals were of the analytical grade and were used as received without any further processing.

6.2.2 Hydrothermal Synthesis of UCP

ITO, FTO & plain Silica glass (P.G.) substrates (1.5cm x1.5cm) were dipped in a hot (50 ^oC) nitric acid (HNO_3) solution for 15 minutes. Successively substrates were rinsed with deionized water and acetone 2-3 times for removing organics/other impurities. Next, pre-processed substrates were etched by exposing them to H.F. solution for 5 seconds (ITO and FTO) and 20 seconds (P.G. substrate). After repeated washing and drying, all substrates were readied for further solution-phase processing. The $NaYF_4:Yb^{3+}$, Tm^{3+} Upconverting phosphors (UCP) were prepared by vigorously mixing 0.83 M NaF (60%) and 0.2 M each of $YCl_3.6H_2O$ (16%), $YbCl_3.6H_2O$ (3.4%), $TmCl_3.6H_2O$ (0.6%) and CA (20%) at room temperature for 30 minutes, until white translucent solution was obtained. Then the entire mixture was transferred to a

Teflon-lined stainless steel autoclave, with a specific substrate (ITO/FTO/PG) dipped into the mixture and allowed to react hydrothermally by maintaining the hot plate temperature at 215 ^{o}C for 10h. After completion of the reaction, the autoclave was cooled down to room temperature and collected solution subjected to multiple washing by repeated sonication and centrifugation steps. The final collected UCP was dried overnight at 75 ^{o}C and stored.

The different UCP prepared by a synergistic combination of other chelating ligands and substrates are addressed according to the terminology mentioned in table 6.1 throughout the manuscript.

Table 6.1 The nomenclature adopted for several described UCP in the current experiment.

Chelating agent	Substrate	Nomenclature
EDTA	ITO/FTO/PG	UCP _EDTA@ITO /UCP _EDTA@FTO /UCP _EDTA@PG
EGTA	ITO/FTO/PG	UCP _EGTA@ITO /UCP _EGTA@FTO /UCP _EGTA@PG
DTPA	ITO/FTO/PG	UCP _DTPA@ITO /UCP _DTPA@FTO /UCP _DTPA@PG

6.2.3 Characterization

Morphology and size of the different UCP were analyzed using scanning electron microscopy (FEI NOVA NANOSEM 450, U.S.), whereas phase and crystallinity were investigated through an X-Ray diffractometer (XRD) (Rigaku Smart Lab diffractometer, Miniflex having CuKα radiation with λ=1.54 Å). Further, the emission property of UCP was recorded using a spectrofluorometer (Quanta Master-400, PTI, CANADA)) mounted with a

continuous wave (C.W.) 980 nm diode laser (MD-III-980-2W; power density used ~ 3.5 Wcm^{-2}) at a step size of 1 nm, slit width of 0.5 nm integration time of 0.1s.

6.3 Result & Discussion

6.3.1 XRD Analysis

The XRD patterns (Fig. 6.1) revealed that the UCP prepared by a synergistic combination of substrates and chelating agents are highly crystalline in nature, mostly present in the hexagonal (β) phase (JCPDF card no. 28-1192). Some mixed phases Upconverting crystals are also reflected. UCP produced using a combination of EDTA as a chelating agent and P.G. or ITO (Fig. 6.1a & 6.1c) as a substrate is found to be in mixed-phase [cubic (JCPDF card no. 77-2042) + hexagonal], with a significant content of cubic (α) phase present in them. However, in the case of FTO substrate (Fig. 6.1b), the prepared UCP is in perfect hexagonal phase with a high degree of crystallinity (Table 6.2), supported by close matching with a standard hexagonal pattern of the $NaYF_4$ system. The further appearance of the peak corresponding to 38.03 and 56.13^o suggests unreacted NaF (JCPDF card no. 98-004-8929) in diffraction pattern probably originated due to excess amount of precursor initially taken during synthesis and not any kind of decomposition product due to the absence of peak corresponding to YF_3. As NaF is the principal constituent of $NaYF_4$ host lattice and is responsible for the photon-phonon interaction, it was taken in ~4 times in excess quantity compared to the YCl_3 precursor. This would compensate for the losses incurred during longer duration solution-phase processing and play an essential role in controlling phase and morphology UCPs through the acceleration of the crystallization process [389-391]. The

excess amount of NaF resulting in precipitation during solution-phase processing is thus visible in the diffraction pattern. However, Yb^{3+} and Er^{3+} are dopants and present in small amounts not visible in the x-ray diffraction peaks.

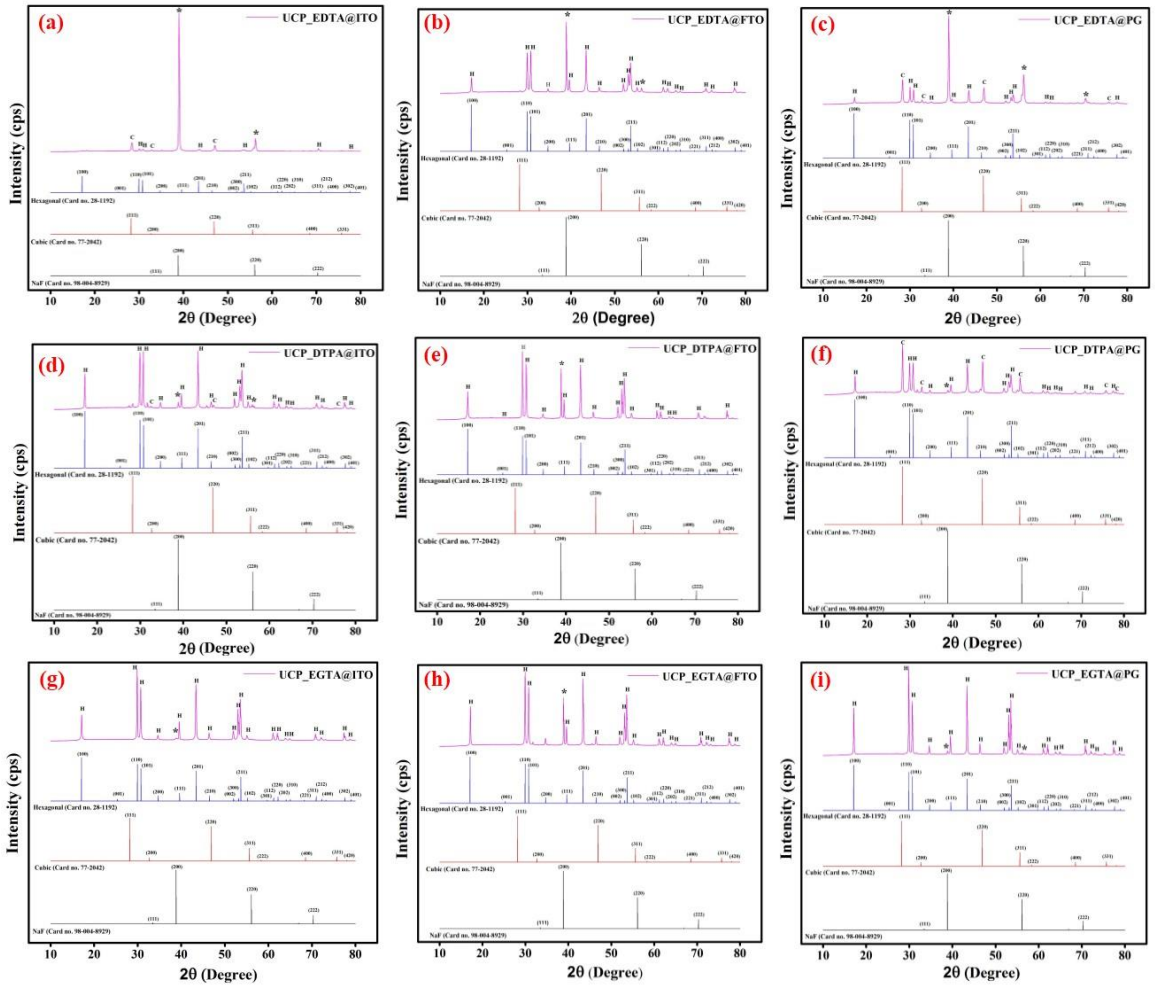

Figure 6.1 XRD analysis of UCP by different combination of chelating agent and substrate. (a)UCP_EDTA@ITO, (b) UCP_EDTA@FTO, (c) UCP_EDTA@PG, (d) UCP_DTPA@ITO, (e) UCP_DTPA@FTO, (f) UCP_DTPA@PG, (g) UCP_EGTA@ITO, (h) UCP_EGTA@FTO, (i) UCP_EGTA@PG

In the case of DTPA as a chelating agent, the Plain glass (P.G.) substrate has led to the development of mixed-phase UCP with a high cubic to the hexagonal ratio (~3) and

negligible traces of NaF impurity. The majority of the Upconverting crystals are aligned in (111) plane of the cubic phase (Fig. 6.1f). Whereas ITO and FTO substrate assisted synthesis (Fig. 6.1d & 6.1e) formed highly crystalline β-phase (Table 6.2) of $NaYF_4$:Yb^{3+}, Tm^{3+} phosphors with impurity peak at 38.03^o due to unreacted NaF. Also, it is observed from the XRD pattern that most of the synthesized crystals are preferably oriented along (100), (110), (101), (201), and (211) planes of hexagonal symmetry.

For EGTA assisted synthesis (Fig. 6.1g-i), interestingly, all the substrates resulted in Upconverting crystals that have a high degree of crystallinity (~ 61 %), with the majority of the Upconverting crystals grown along the (110) and (201) crystal plane. Also, a hexagonal phase has a very high growth rate than a developed cubic phase resulting from a negligible cubic/hexagonal ratio (~ 0.004).

Overall all the diffraction patterns have a tinge of NaF impurity whose intensity changed with variation in the substrate and chelating agent. It can be correlated with coordinating capability of chelating ligands for rare-earth ions and subsequent precipitation of surplus amount of NaF precursor as earlier mentioned. Octadentate DTPA ligand having high formation constant as compared to EDTA and EGTA, chelates better with Re^{3+} ions. However, it is worth noting that the chelation nature of DTPA is only effective under an acidic medium [392]. Moreover, EDTA a hexadentate ligand with cyclically oriented coordination capability has the best chelation ability under basic medium. Since the synthesis was carried out under slightly alkaline conditions, which is directly related to the solubilization process of chelating ligands, EDTA might have acted as the best coordinating ligand [392]. During synthesis, improved chelation of Re^{3+} ions and subsequent bond

weakening results in primary nucleation followed by crystal growth and stabilization. Thus, rapid nucleation and subsequent stabilization of resulting crystals during UCP synthesis might result in more unconsumed NaF precursors reflected in the X-ray diffraction pattern.

The average crystallite size 'D' of prepared UCP was calculated according to the Scherrer equation as represented in equation 1 and represented in table 6.2.

$$D = k*\lambda/\beta*\cos\theta \qquad (1)$$

D = Crystallite size (nm), k = 0.9 (empirical constant related to shape factor), λ = 0.15406 (wavelength of for CuKα radiation), β = FWHM for the diffraction peak (radian unit), θ = half of the Bragg angle (radian).

Table 6.2 shows that, on average, EDTA chelating ligand is responsible for developing small-sized Upconverting crystals.

6.3.2 Effect of lattice strain on crystallographic property

As mentioned earlier, hydrothermal synthesis has a significant role in inducing lattice strain in synthesized crystal structures [375]. Therefore UCPs synthesized in this study are subjected to lattice distortion catalyzed by internal strain. This need to be investigated carefully while calculating crystallite size from the Scherrer equation. It is important to mention that lattice distortion has an implicit role in XRD peak broadening that affects the calculated crystallite size [393]. Also, resulting crystallite size reduction is also responsible for releasing lattice strain and peak broadening [374].

Since crystallite size and lattice strain are responsible for line broadening of diffraction peaks [394], hence to get an accurate estimation of crystallite size and associated strain with diffraction peaks “Williamson-Hall” equation was adopted.

Table 6.2 Degree of crystallinity, lattice strain and associated crystallite size of synthesized UCP

Sl No.	UCP	Crystallite Size (D) (Scherrer Equation) (nm)	Crystallite Size (D) (WH equation) (nm)	Lattice Strain (Ɛ) (a.u.)	% Hexagonality	$I_{(111)/(100)}$ (Cubic/Hexagonal)
1	DTPAITO	35.15 ± 11.20	39.50	4.29E-4	52.10	0.178
2	DTPAFTO	37.67 ± 6.09	43.32	3.27E-4	57.32	0.0176
3	DTPAPG	31.03 ± 7.86	38.19	6.83E-4	48.63	3.06
4	EDTAITO	26.24 ± 8.36	25.39	7.54E-5	12.05	13.71
5	EDTAFTO	32.09 ± 7.29	37.27	6.12E-4	50.86	0.104
6	EDTAPG	29.01 ± 8.93	73.75	0.00274	28.14	5.36
7	EGTAITO	33.90 ± 8.26	44.72	9.37E-4	61.75	0.007
8	EGTAFTO	39.06 ± 5.63	55.46	6.79E-4	58.03	0.004
9	EGTAPG	40.22 ± 5.78	56.82	4.58E-4	58.93	0.011

Total peak broadening is the function of broadening due to crystallize size and broadening due to micro-strain.

$$\beta_T = \beta_D + \beta_\varepsilon \quad (2)$$

β_T = Total peak broadening, β_D = broadening due crystallite size, β_ε = broadening due to micro-strain.

Induced strain effect on line broadening (β_ε) can be described as:

$$\beta_\varepsilon = 4\text{Ɛ}*\tan\theta \quad (3)$$

Where Ɛ = lattice strain. Now equation 2 can be modified by putting the values of equations 1 and 3 and represented as,

$$\beta_T = k*\lambda/D*\cos\theta + 4\text{Ɛ}*\tan\theta \quad (4)$$

On multiplying both sides by cosθ equation, 4 now can be modified as:

$$\beta_T*\cos\theta = k*\lambda/D + 4\text{Ɛ}*\sin\theta \quad (5)$$

Linear fit of above expression results in crystallite size as well as associated lattice strain in X-ray diffraction pattern from the intercept and slope respectively (Fig. 6.2). It is important to mention here that a uniform tensile and compressive strain (Macro strain) results in the shifting of diffraction peaks. In contrast, a non-uniform strain is responsible for diffraction line broadening [380].

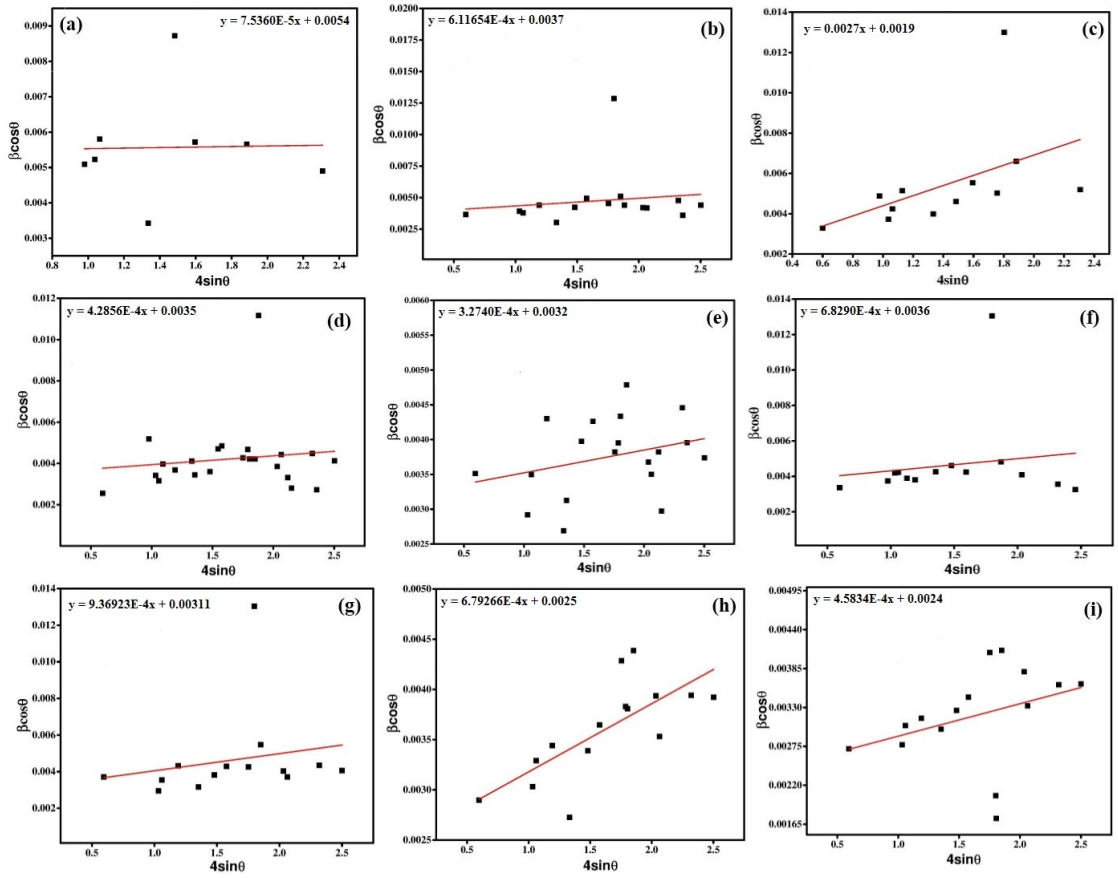

Figure 6.2 Williamson-Hall analysis of UCP. (a)UCP_EDTA@ITO, (b) UCP_EDTA@FTO, (c) UCP_EDTA@PG, (d) UCP_DTPA@ITO, (e) UCP_DTPA@FTO, (f) UCP_DTPA@PG, (g) UCP_EGTA@ITO, (h) UCP_EGTA@FTO, (i) UCP_EGTA@PG.

Since hexagonal peaks are dominated in the diffraction pattern, hence they have a major influence on the plot of the Williamson Hall (W.H.) equation. In the current scenario, there is a scattering of data points from the linear fitted region of W.H. equation; there exists anisotropy in the developed Upconverting systems, and both crystallite size and lattice strain are responsible for diffraction line broadening. Uniform distribution of lattice strain and particle size has a strong influence on linearizing the W.H. equation. From figure 6.2, it is clearly visible that there is a minimum scattering of data points from the linear fitted

line of the W.H. equation for UCP_EDTA@ITO, UCP_DTPA@ITO, UCP_DTPA@PG, and UCP_EGTA@FTO; hence these are subjected to uniform strain during their growth.

From table 6.2, it is clearly visible that, while using DTPA as the chelating agent, the Upconverting crystallites generated in the presence of conducting glass substrate (ITO, FTO) are larger in comparison to synthesis involving plain glass (P.G.) substrate. It can be correlated with the calculated overall lattice strain mentioned in table 6.2. Plain glass-assisted synthesis, developed lattice strain in prepared UCP, high as compared to ITO and FTO mediated synthesis. Hence to reduce the above-generated strain, lattice relaxation occurred, and small-sized crystals were produced. Interestingly in the case of synthesis of UCP using EDTA as chelating ligand, there is no clear cut ordering between crystallite sizes produced and lattice strain developed by the synergistic combination of conducting or non-conducting substrates. The EDTA-ITO-assisted synthesis produces a lesser lattice strain that can be interlinked with very weak Upconverting crystal growth (Fig. 6.1a).

Moreover, the diffraction peak mainly comprises impurity arising from unconsumed NaF, ultimately generating the least amount (~ 12%) of hexagonal crystals. Hence strain developed in resulting Upconverting crystals were less along with small crystallite size also resulted. Whereas EDTA-FTO assisted synthesis by virtue of lesser lattice strain compared to EDTA-PG assisted synthesis resulted in large crystallite size. Abrupt increment of lattice strain in EDTA-PG assisted synthesis may result from a greater percentage of cubic phase growth than that of hexagonal phase (NaF contribution can also be included). The cubic phase has a possible role in inducing compressive strain within expanding lattice of nucleating hexagonal phase, ultimately enhancing the overall lattice strain. This unprecedented rise is also related to the close-fitting of with linear equation of

the W.H. plot. Williamson-Hall equation also predicts a very high crystallite size value, unlike the Scherrer equation, due to unwanted rise in lattice strain and crystals associated with two equally reflected phases. Unlike DTPA and EDTA, EGTA assisted synthesis irrespective of substrate used for UCP synthesis produced crystallite size with comparable values. This may be correlated with a nearly similar magnitude of lattice strain generated in them and a high degree of hexagonality in produced crystals. Hence the choice of substrate-chelating agent combination has an important role in controlling the crystallite size of UCPs prepared.

There is a difference in crystallite size of UCPs estimated from Scherrer and W.H. equation as represented in Table 6.2. This difference can be explained because the micro-strain can induce a more significant broadening in the diffraction peak, whereas the full width of the diffraction peak is used in crystallite size calculation. Indeed the W.H. equation provides correctness to the above-shouted problem [395].

Ghosh et al. [378] reported that crystal dislocation related to lattice strain has a major influence on diffraction line broadening at low Braggs angle. Hence to observe the possible effect of lattice strain on diffraction peak broadening and subsequent determination of crystallite size, major hexagonal peaks grew along (100) crystal plane are investigated carefully. This observation also has a crucial role in ascertaining the underlying mechanism associated with the growth of Upconverting crystals and subsequent morphology tuning by variation of chelating agent and substrate used during synthesis.

6.3.3 SEM Analysis and Particle size distribution

Bulk phase Upconverting phosphors (UCP) synthesized hydrothermally by the synergistic combination of substrate and chelating ligands were characterized through scanning electron microscopy, and the resulting morphology and particle size distribution are described below. It is observed from figure 6.3 that there is variation in the morphology (shape and size) of Upconverting crystals synthesized by different combinations of substrate and chelating agent. Moreover, due to the overall positive strain developed within the UCP during the growth process, all reported particles (Fig. 6.3) were subjected to lattice expansion, leading to nearly elongated morphology. Furthermore, when chelating agents were varied prominent changes in the morphology of UCPs morphology was observed. For example, the nearly cube-shaped UCP gradually changes to hexagonal micro-prism and micro-rod structure when the chelating agent was changed from EDTA to DTPA and then to EGTA indicating the major role of chelating agent in tuning the morphology of UCP as compared to the substrate. However, the role of substrate charge in modulating the morphology cannot be overruled due to changes in parameters related to the size and shape of UCP. The surface charge over the substrate is known to accelerate/ control/ crystal growth and morphology [396]. In fact, the particles grown over substrates have a similar kind of morphology as bulk phase material (*Appendix* D1). Thus there may be a multifaceted way of particle growth directed from substrate to bulk phase or vice-versa.

Though there is no reported relation between particle size and corresponding strain associated with parent crystals. Here an attempt to correlate particle morphology with lattice strain has been made. The particle size distribution study (*Appendix D2* & Table

6.3) reveals that EDTA assisted UCP on average produced smaller-sized particles, irrespective of the type of substrates employed. This may be directly related to the improper growth and smaller crystallite size obtained from the Scherrer equation. Alternately, we can presume that the greater content of the cubic phase (Table 6.2) put forward a balancing mechanism for the particle growth process. The tensile strain, associated with the hexagonal phase, is responsible for crystal expansion ultimately compressed by the cubic phase growing within. However, the positive rate of particle size growth with a rise in lattice strain in the case of EDTA assisted synthesis requires further investigation. In the case of DTPA assisted synthesis over the plain glass (P.G.) and ITO substrate, UCP with smaller sizes: 1.9 and 2 μm respectively, resulted, unlike FTO (~2.5 μm) assisted synthesis (Table 6.3). This may have been caused due to the low value of lattice strain (3.27E-4) in FTO mediated synthesis, resulting in the formation of large crystallite size. The lattice strain in the case of FTO was found to be noticeably smaller than the P.G. (6.83E-4) and ITO (4.29E-4). For EGTA assisted synthesis, comparable values of lattice strain (Table 6.2), respectively, might have resulted in UCP with similar sizes (FTO ~3.7 μm and P.G. ~2.3 μm). On the contrary, for ITO assisted UCP, a high value of lattice strain (9.37E-4) led to a smaller particle size of ~1.7 μm (Table 6.3).

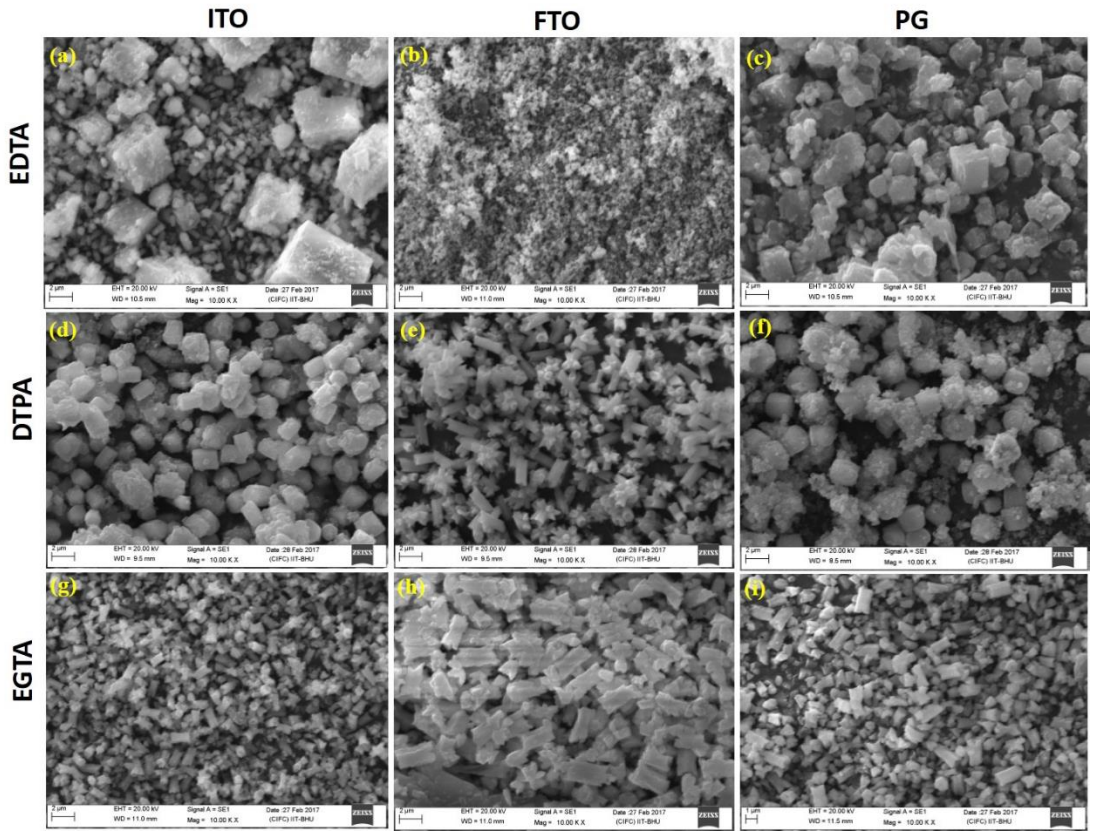

Figure 6.3 Scanning electron micrographs of UCP. (a)UCP_EDTA@ITO, (b) UCP_EDTA@FTO, (c) UCP_EDTA@PG, (d) UCP_DTPA@ITO, (e) UCP_DTPA@FTO, (f) UCP_DTPA@PG, (g) UCP_EGTA@ITO, (h) UCP_EGTA@FTO, (i) UCP_EGTA@PG

Since the chelating agent has a prominent role in controlling the morphology of UCPs, there should be a mechanistic approach to study the correlation as mentioned above. Generally, improved chelation capability of the ligand towards specific ions in precursor solution increases the energy barrier needed for nucleation; hence, those ligands having strong chelation capacity require higher thermal conditions for crystallization [397]. It is noteworthy that the UCPs grown in association with different substrates are in prismatic micro-rod, micro-cube, hexagonal micro-prism, and nanosphere-like shapes using various chelating ligands. The UCPs formed by using EDTA ligands are most uneven morphology mainly comprised of spheres or micro-cubical shaped particles. Uneven

morphology may be due to the comparable formation amount of two major phases in prepared UCP. Also, synthesis using EDTA as a chelating agent in the presence of all substrates results in unreacted fluoride content as observed from the intense diffraction peak of NaF in the XRD pattern (Fig. 6.3a-c) with a small intensity of NaF in the presence of FTO substrates. While largest in the case of ITO, which indicates an incomplete separation of nucleation and growth processes, thus leading to the development of most non-uniform UCP using ITO substrates followed by the P.G. substrate [398]. Small-sized spherical/cubical/prismatic micro-rod morphology can be correlated with the small molecular weight and less complex structure of ligand compared to EGTA and DTPA. Generally, ligand dynamics over the crystal surface have a strong tendency of controlling the growth of $NaYF_4$: Yb^{3+}, Tm^{3+} by coordination effect [399]. Hence a hypothesis can be proposed from surface adhered ligand dynamics for the development of several particle morphologies. The DTPA ligand is an expanded version of EDTA, based on a Diethylene triamine backbone with five carboxymethyl groups. Similarly, EGTA is an aminopolycarboxylic acid as of EDTA but has an elongated structure due to additional R-O-R linkage. This makes EGTA and DTPA more complex and heavier moieties as compared to EDTA.

Table 6.3 Particle size distribution of UCP synthesized

Sl No.	UCP	Particle Size (μm)
1	DTPA@ITO	2 ± 0.1
2	DTPA@FTO	2.55 ± 0.21
3	DTPA@PG	1.9 ± 0.2
4	EDTA@ITO	0.88 ± 0.17
5	EDTA@FTO	0.34 ± 0.05
6	EDTA@PG	0.71 ± 0.24
7	EGTA@ITO	1.71 ± 0.1
8	EGTA@FTO	3.70 ± 0.3
9	EGTA@PG	2.3 ± 0.2

Generally, a smaller ligand tends to leave the crystal surface rapidly during hydrothermal synthesis, facilitating non-directional growth aligned along a different crystallographic axis. This is clearly visible in the case of UCP synthesized by EDTA using various substrates depicting nearly spherical/cubical morphology with an aspect ratio close to unity. Smaller-sized particles are also formed due to the improved and rapid chelation capability of EDTA, as mentioned earlier. The aggregated structure of UCP in the case of EDTA might have resulted due to faster leaving chelating agents from crystal facets, thus making their surface unstable. Whereas, in the case of DTPA and EGTA, due to large molecular structure, the tendency to leave crystal facets became slower Instead, growth took place along a certain crystallographic axis (C-axis) forming micro-rod or hexagonal micro-prism assembly with aspect ratio deviating from unity. The directional

growth in the case of DTPA and EGTA assisted synthesis can be ascertained from the fact that, in their diffraction pattern, the most intense peak observed for growth along the major hexagonal plane, unlike EDTA assisted synthesis. Moreover, due to the nearly comparable molecular backbone of the chelating agent and almost complete separation of nucleation and growth process based on negligible fluoride residue, there is no distinct morphological difference between the UCP synthesized using DTPA & EGTA chelating agent. Also, there is the formation of nearly monodispersed morphology of UCP. Additionally, the unstable surface dynamics of crystals during their dissolution in the reaction media results in the formation of a few irregular morphologies. Delayed detachment of ligands from growing crystal facets in DTPA assisted synthesis, pertaining to large size effect formed flower-like aggregation on the subsequent growth process. After a certain growth, the extrusion process might have produced micro-rod assembly.

The most important factor responsible for the morphology assessment of the developed Upconverting crystals is the crystallographic phase of the initial seed formed. Characteristic cell structures related to the crystalline phase of the seeds strongly affect the further growth process. Since in our developed Upconverting system there is the formation of both α and β phase during the growth of Upconverting crystals, morphology variation is observed. Generally, the cubic (α) phase of $NaYF_4$ seeds has isotropic unit cell structures, inducing the isotropic growth of particles, unlike its hexagonal (β) counterpart with anisotropic unit cell ultimately yielding particles with anisotropic morphology (e.g., hexagonal structure). For EDTA assisted synthesis, as the diffraction pattern consists of a higher entity of cubic phase, spherical nanoparticles, and micro-cubic structure (aspect ratio ~1) is resulted for prepared for Upconverting crystals to minimize the surface energy associated with crystal facets. Small quantities of rod-shaped

morphology are also observed by virtue of developing hexagonal phase during EDTA assisted synthesis. On careful observation, it is found that on using DTPA and EGTA as chelating agents, uniform hexagonal prismatic micro-rods and micro-prisms were obtained. This is likely due to the formation of a higher percentage of hexagonal phase yield. Generally, the hexagonal prismatic micro-rod and micro-prism structures are interchangeably formed by orienting the final growth direction based on the restrictive movement of adhered chelating ligand to the developing crystal facets. Whereas, hexagonal prism or micro-rods, the top or bottom planes have {0001} surface while prismatic side planes are denominated as (10I0), (I010), (0I10), (0I10), (1I00), and (I100). In the case of DTPA@FTO mediated synthesis, long and uniform hexagonal prismatic micro-rods are obtained (Table 6.3) owing to the higher percentage of hexagonal phase in the presence of the FTO substrates. Whereas, in the case of ITO and P.G. substrate-assisted synthesis, small-sized hexagonal micro-prisms resulted in few quantities of cubic nanospheres topped over these microstructures consistent with a low proportion of hexagonal phases accompanied with cubic impurity also observed in the diffraction pattern. From these observations, we can presume that the chelating capability of DTPA is hindered during simultaneous growth of cubic phase, and crystal growth is restricted along [0001] direction to produce small-sized hexagonal micro-prism morphology. However, in FTO mediated synthesis, a greater percentage of hexagonal phase (Table 6.3) display a higher affinity of DTPA ligand towards energetic side planes [{10I0} equivalent] of a prism. Which ultimately drives the growth along the c-axis [0001] direction leading to the formation of prismatic micro-rod shaped UCP. Further, hexagonal micro-prisms and micro-rods produced are perfectly uniform and monodispersed. The average diameter of the micro-prisms is prominent in the case of P.G. substrate (~ 2.17

μm) as compared ITO (~ 1.49 μm) and FTO (~ 1 μm) while the length increases from 1.9 to 2.55 μm. This finding indicates strong adsorption of DTPA ligand onto the (0001) facets as far as P.G. and ITO substrate are concerned. Besides, DTPA (chelating agent) deposition on the six equivalent (10I0) prismatic side planes in case of FTO substrate accelerates growth velocity along (0001) direction. Hence hexagonal micro-prism and micro-rod assembly are formed in former and latter substrates, respectively. Also, we can postulate that the evolution of the cubic phase in addition to the hexagonal phase significantly inhibits the preferred growth along with the [0001] direction and subsequently enhances the sideway growth, thus leading to the formation of a mixture of 2D hexagonal prism and spherical nanoparticles on top of it.

Similarly, due to the higher degree of crystallographic hexagonal phase, EGTA mediated UCP are hexagonal prismatic micro-rod in shape irrespective of the substrate used, unlike the other two chelating ligands. For EGTA assisted growth, ITO substrate yielded the most uniform and monodispersed prismatic micro-rods followed by FTO substrate, corroborating a high degree of hexagonality in them. The micro-rods obtained using the P.G. substrates are not completely intact in shape, broken and non-uniform pertaining due to slight cubic impurity in it. Moreover, the absence of well-defined particle morphology in the case of EGTA assisted synthesis owing to the high degree of hexagonal crystallinity and intense hexagonal phase of growing seed for all the samples.

In a simplistic approach, morphology tuning through variation of chelating ligand can be postulated from the X-ray diffraction pattern of prepared UCP. Growth of the major hexagonal phase is prominent along the (100/110) plane for EGTA and DTPA assisted synthesis. While for EDTA assisted synthesis, these peaks are less developed. Generally,

chelating agents capped on the highly energetic facets of developing crystal to orient growth along with other directions [400]. Since the developing crystal facets are oriented along X/Y plane in EGTA and DTPA assisted synthesis, the particle growth at subsequent stages are directed along Z-direction, ultimately resulting micro-rod type morphology (Fig. 6.3d-i). However, due to simultaneously developing cubic phase (though in lesser concentration), the unidirectional growth was also restricted to some extent, as reflected from broken hexagonal micro-prism and micro-rod type morphology with aspect ratio deviating from unity. In the case of EDTA assisted significant synthesis amount of cubic phase formed in parallel to hexagonal phase. The major peak corresponding to the cubic phase is oriented along the (111) plane, unlike EGTA/DTPA assisted synthesis. Thus due to the capping effect the growth is hindered from all directions, or there was non-directional growth in subsequent stages, ultimately developing small-sized spherical or cubical particles along with particles with uneven morphology. Improved chelation capacity of EDTA may have been reflected from the multiaxial compressed particles. Whereas less effective chelation capability of DTPA and EGTA assisted, synthesis may be correlated with the fact that there is no 100% uniaxial growth.

Furthermore, the size distribution analysis discussed earlier also provides an insight into the various factors controlling the UCPs growth in the presence of chelating ligands. The scanning electron microscopy results revealed micron-sized particles with varying morphology, grown in the presence of conducting/non-conducting substrates, depending upon the chelating ligand used. The EGTA and DTPA ligand produced large-sized particles as compared to EDTA assisted synthesis. Small-sized UCPs resulting from EDTA assisted synthesis may be interlinked with the simple molecular structure of EDTA, which has a tendency of stabilizing small-sized nuclei formed during the initial

phase of synthesis. These surface stabilized nuclei have a weaker tendency of dissolution in the hydrothermal reaction mixture, thus inhibiting the growth of large-sized nuclei during the subsequent crystallization process. The size anisotropy in the case of EDTA assisted synthesis also resulted due to the formation of two major phases mentioned previously. Similarly, bulkier DTPA/EGTA facilitates aggregation of nuclei during the crystal growth process as small nuclei are not stable. Hence improved surface dynamics as well as large-sized nuclei helped in the formation of bigger sized UCPs.

Since the Upconversion system exhibits a larger fraction of hexagonal phase over the cubic phase, we systematically investigated characteristic diffraction peak corresponding to hexagonal phase located at 17.12^{o} corresponding to (100) plane. It can provide a generalized overview for morphology tuning through variation of strain developed in the crystal lattice by the synergistic combination of chelating agent and substrate during synthesis of UCP. In the case of EDTA assisted synthesis, the Bragg's peak corresponding to 17.12^{o} is red-shifted in all the reported UCP (Fig. 6.4a). The peak corresponding to UCP_EDTA@ITO is shifted maximum to a higher degree, indicating prepared crystals are subjected to more uniform strain [401]. As a result there is a contraction of developed crystals [402], which breaks down big chunks of particle to result a number of small-sized cubes. However, in the case of UCP_EDTA@PG and FTO there is not much significant shift in peak position, but peak broadening is quite visible. Hence both may be subjected to more non-uniform compressive as well as tensile strain, producing irregular morphology. For DTPA assisted synthesis, e.g., UCP_DTPA@PG and ITO, the reported low angle diffraction peak (Fig. 6.4b) is subjected to broadening as well as red shifting. Hence the micro-rod structure formed initially probably compressed uniformly from all directions and maintain its morphology intact. Whereas

in the case of UCP_DTPA@FTO the peak position remains unchanged, and due to the symmetric nature of the observed diffraction curve, it tends to non-uniform tensile as well as compressive strain. Lattice parameters are expanded to maintain the micro-rod morphology, but simultaneous contraction leads to breakage and inter-coupling. Interestingly for all the UCP synthesized by the combination of EGTA ligand and substrates, there is nearly no shift in peak position (Fig. 6.4c) but broadened due to non-uniform lattice strain. For UCP_EGTA@FTO the shift in peak position towards the right may positively impact its elongated morphology, which is relatively under uniform compressive strain, and its structure remains intact. Whereas for UCP_EGTA @PG and ITO, under non-uniform compressive as well as tensile strain resulted in broken micro-rod morphology. Clearly saying all such observations are preliminary, rigorous analysis required for exact estimation underlying hypothesis related to morphology control.

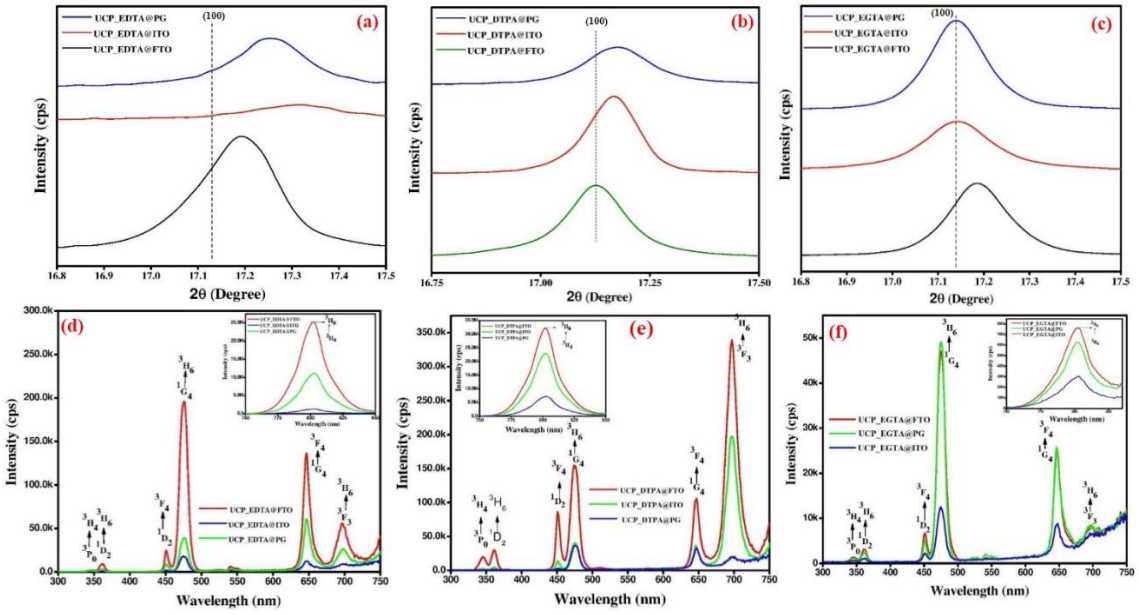

Figure 6.4 Low angle peak shift in UCP synthesized using (a) EDTA, (b) DTPA, (c) EGTA chelating ligand in association with various substrates. Upconversion luminescence intensity from UCP synthesized using (d) EDTA, (e) DTPA, and (f) EGTA chelating agent.

6.3.4 Photoluminescence spectra

The luminescence spectra of UCP prepared by different combinations of substrate, and chelating agents are represented in figures 6.4d-f. The major peaks of luminescence spectra obtained are centered at 345, 360, 450, 475, 645, 700 nm corresponding to ($^3P_0 \rightarrow {}^3H_4$), ($^1D_2 \rightarrow {}^3H_6$), ($^1D_2 \rightarrow {}^3F_4$), ($^1G_4 \rightarrow {}^3H_6$), ($^1G_4 \rightarrow {}^3F_4$), ($^3F_3 \rightarrow {}^3H_6$) transitions respectively occurring due to the Upconversion process. In addition to an additional peak corresponding to 800 nm ($^3H_4 \rightarrow {}^3H_6$) also resulted, the intensity of which is very much high compared to characteristics emission spectra of Tm^{3+} doped Upconverting system. This spectrum is responsible for the heat generation ability of prepared UCP due to the non-radiative transition process. Hence, prepared UCP microstructures can be used in biomedical applications like cancer theranostics and analyte sensing if proper morphology and surface functionality are controlled through rigorous experimentation. The tuning of Upconversion luminescence intensity is the function of several factors such as degree of hexagonality, development of lattice strain, etc. In the case of EDTA assisted synthesis, very weak hexagonal crystallinity (~12 %) resulted in diminishing luminescence intensity for ITO substrate. However, in between P.G. and FTO substrate, the latter is responsible for improved luminescence intensity pertaining to the small value of lattice strain and a high degree of hexagonality (~51%). If the characteristic luminescence intensity corresponding to 475 nm is considered, the rise in intensity is observed close to be 5 times. PG assisted synthesis resulted weak emission intensity also due to formation of greater amount of cubic phase [$I_{(111)/(100)} = 5.36$] as compared to FTO [$I_{(111)/(100)} = 0.104$] based system. Similarly, in DTPA assisted UCP synthesis, FTO as a

substrate resulted in maximum luminescence intensity due to a lesser amount of lattice strain (3.27E-4) compared to ITO and P.G. with micro-strain observed to be 4.29E-4 and 6.83E-4, respectively. Precisely saying the characteristic emission corresponding to 475 nm wavelength for UCP_DTPA@FTO is ~4 times high with respect to UCP_DTPA@PG and UCP_DTPA@ITO. Moreover, P.G. and ITO substrate assisted UCP have comparable luminescence intensity due to a similar degree of hexagonality (~55 %). In EGTA assisted comparable synthesis amount of hexagonal crystallinity (~60 %) resulted in equal magnitude of Upconversion luminescence intensity in the case of UCP corresponding to 3 mentioned substrates. However, due to the high value of lattice strain (9.37E-4) in ITO assisted synthesis in comparison with FTO (6.79E-4) and P.G. (4.58E-4), weak Upconversion intensity results. The corresponding emission at 475 nm for UCP_EGTA@ITO is 3.5 times less than UCP_EGTA@PG and UCP_EGTA@ITO.

As earlier mentioned, the developed lattice strain in the Upconverting crystal has a significant role in modulating its luminescence property [403]. With the increase in lattice strain, luminescence is quenched by the rise in non-radiative relaxation pathways. One of the important factors in enhancing luminescent character is decreasing the associated phonon quenching of the host matrix, catalyzed via an increase in the rate of energy transfer between host ion and doped rare-earth ions. Energy transfer between host Y^{3+} ion or Yb^{3+}-Tm^{3+} ion is favorable via phonon energy coupling [377], which depends upon reduction in interionic separation. By reducing the lattice strain, the separation distance between the Y^{3+} ion or Yb^{3+}-Tm^{3+} ions, reduced and hence increased rate of energy transfer suppresses the luminesce quenching process, ultimately resulting in high quantum efficiency. This process is comparable to distorting the crystal field symmetry around doped rare- earth ions, leading to easing of "Laporte selection rule" to increase

the luminescence intensity. Same can be observed in the case of synthesized UCP via synergistic combination of substrates and chelating ligands. Less lattice strain value has positive influence on luminescence behavior as mentioned previously. Lastly, the modulation of Upconversion intensity through different chelating ligands and substrates needs to be investigated further for obtaining UCP with desired morphology and optical characteristics.

6.4 Conclusion

In conclusion, a facile one-pot method is developed to synthesize highly crystalline UCPs of variable shape (micro cubes, small sphere, hexagonal micro-prism and micro-rod) and with wide size ranges. Prepared UCPs with a high degree of hexagonal crystallinity and emission intensity are developed by a synergistic combination of substrates and chelating agents with varying nature and molecular structure. A mechanistic approach has been adopted to underlay the interlinked mechanism between crystallinity, lattice strain, particle morphology, and emission intensity. Substrates used in the synthesis responsible for inducing strain in the developed crystal lattice, which along with chelating ligand coordinates the formation of hexagonal UCPs diverse morphology. Infact degree of crystallinity and lattice strain are found to be crucial parameters for maximization of the Upconversion intensity. No external treatment or post synthetic reaction needed to synthesize UCP of desired morphology, crystallinity and emission property. EDTA assisted synthesis resulted small sized UCPs with FTO substrate responsible for maximization of Upconversion emission. Overall DTPA mediated synthesis pertaining to large hexagonal crystals; low intrinsic lattice strain resulted in augmented Upconversion emission. Moreover, tuning of Upconversion intensity through variable

crystallographic formation and size adjustment by suitably choosing chelating ligands and substrates of different nature during synthesis is the first of its kind.